Hindered Rotation along Carbon–Nitrogen Bonds. The Effect of Carbonyliron in Complexes of 7-Azanorbornadiene Derivatives†

Tahsin J. Chow,*[a,b] Jiunn-Jye Hwang,[c] Yuh-Sheng Wen[a] and Su-Ching Lin[a]

[a] *Institute of Chemistry, Academia Sinica, Taipei, Taiwan, Republic of China*

[b] *Department of Chemistry, National Chung-Cheng University, Chia-Yi, Taiwan, Republic of China*

[c] *Department of Chemistry, National Taiwan University, Taipei, Taiwan, Republic of China*

Hindered rotations have been observed for certain *N*-substituted 7-azanorbornadiene (7-azabicyclo-[2.2.1]hepta-2,5-diene) derivatives and their iron complexes. The free energies of rotation ($\Delta G^{\ddagger}$) have been estimated from the coalescence of NMR signals. The average values found for acetyl amides (**Ib** and **IIb**), benzoyl amides (**IIc** and **IIIc**), and carbamates (**Ia** and **IIIa**) are 17.8, 16.0 and 14.3 kcal mol^{-1} respectively, in accord with electronic effects. For the iron complexes **1**–**4** however, steric factors predominate where the rotations are hindered mostly by the crowding by the ligands. The barriers found for the tetracarbonyliron complexes (**3a**–**3c**) of *ortho*-substituted anilines are proportional to the size of the phenyl substituents, *i.e.* 12.7 kcal mol^{-1} for Me (**3a**), 13.6 kcal mol^{-1} for CN (**3b**), and 14.0 kcal mol^{-1} for I (**3c**). Tricarbonyliron complexes (**2** and **4**) experience a lower barrier to rotation with respect to the corresponding tetracarbonyl ones (**1** and **3**) due to a variation in co-ordination geometry. The energies estimated for the iron carbonyl complexes decrease in the orders **1** (> **Ia**) > **2** as well as **3a** > **4a**. The crystal structures of tetracarbonyl- and tricarbonyl-[1,4-dihydro-1,4-(*o*-tolylimino)naphthalene]iron **3a** and **4a** have been determined.

The kinetics of restricted rotation about the carbon–nitrogen bond in amides has been well studied.[1,2] The barrier to rotation has been found to vary with steric and electronic factors associated with the amide structures. For instance, a better delocalization of the nitrogen lone pair along the N–C=O moiety increases the N–C bond order and therefore hinders the rotation along the bond, while protonation on the nitrogen has an opposite effect. In some cases where the substituents at N are bulky, additional steric factors may become significant.

In our work on iron carbonyl complexes of 7-azanorbornadiene (7-azabicyclo[2.2.1]hepta-2,5-diene) derivatives we have prepared some compounds with *ortho*-substituted aniline moieties. In their ^{1}H NMR spectra certain signals of the ligands coalesce at higher temperature. Although this complies well with the known hindered rotation in nitrogen compounds, it is rather unusual for analogous monosubstituted *ortho*-anilines where rotation about C–N is generally not restricted. The barrier, as observed, must have been introduced by the iron carbonyl moiety. In this report the free energies of activation for rotation about N–C are estimated and compared in terms of structural parameters.

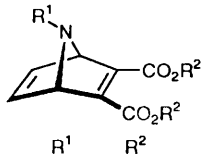

	R^1	R^2
Ia	CO_2Et	Me
Ib	COMe	Me
Id	CH_2Ph	H

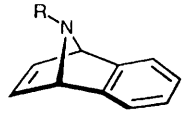

	R
IIb	COMe
IIc	COPh
IId	CH_2Ph

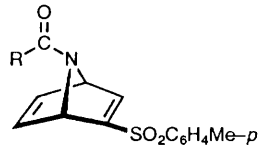

	R
IIIa	OMe
IIIc	Ph

Results and Discussion

Hindered Rotation in 7-Azanorbornadiene Derivatives.—The kinetics of rotation about the N–CO bond of amides can be conveniently analysed by using the variable-temperature NMR technique. The coalescence temperature of the NMR signals is related to the energy of activation. For the *N*-acetyl substituted compound **Ib** and the benzo-fused **IIb** and **IIc** derivatives the rotational barriers are known[2] to be in the range 16.0–18.1 kcal mol^{-1} (Table 1). These values are comparable with those found for dimethylformamide[3] (18.2 kcal mol^{-1}) and *N*,*N*-dimethylbenzamide[4] (15.5 kcal mol^{-1}).

The $\Delta G^{\ddagger}$ for the 2-tosyl-7-benzoyl compound **IIIc** was estimated to be 16.0 kcal mol^{-1}, equal to that of **IIc**. In Fig. 1 the ^{1}H NMR spectra of the bridgehead protons are scanned from 10 to 100 °C. Apparently the two pairs of signals coalesce at 50 °C. For the carbamate derivatives **Ia** and **IIIa** the barriers are measured to be 13.9 and 14.7 kcal mol^{-1} respectively, considerably lower than those of both the acetyl amides **Ib** and **IIb** and the benzoyl amides **IIc** and **IIIc**. The average $\Delta G^{\ddagger}$ for the acetyl amides is 17.8 kcal mol^{-1}, that for benzoyl amides is 16.0 kcal mol^{-1}, and that for the carbamates is 14.3 kcal mol^{-1}. The descending order of acetyl amide > benzoyl amide > carbamate is due to the enhancement of electronic delocalization in the N–CO–R moiety, which reduces the bond order between N and CO. The variation of substituents on the double

† *Supplementary data available:* see Instructions for Authors, *J. Chem. Soc., Dalton Trans.*, 1994, Issue 1, pp. xxiii–xxviii.

Non-SI unit employed: cal = 4.184 J.

bonds of compounds **I**–**III** seems to have little influence on the energy barrier, indicating that the perturbations induced by the substituents, both electronic and steric, are not significant.

It is known that in analogous bicyclic systems the process of nitrogen inversion[5] may proceed at a comparable rate.[2] For certain aziridines, both inversion and hindered rotation are observable within the same temperature range.[6] For the *N*-chloro derivative of **II**, $\Delta G^{\ddagger}$ is reported to be as high as 23.5 kcal mol^{-1}.[7] For *N*-benzyl-substituted derivatives **Id** and **IId** the nitrogen-inversion barriers are reported to be 14.3 and 14.8 kcal mol^{-1} respectively.[2] Comparing the value of **Id** to that of **Ia** (Table 1), it is seen that the nitrogen-inversion barrier in this bicyclic compound is nearly equal to that of the rotation barrier. Nevertheless in our study of **Ia** the processes of rotation and inversion can be distinguished as follows. Below the coalescence temperature, the bridgehead hydrogens of **I** and **II** appear as two sets of signals of equal intensity as a result of the planar symmetry of the molecules. For slow inversion, the intensities of signal pairs are usually non-equivalent but depend on the relative population of invertomers.[8]

Table 1 Spectral parameters and free energies of activation for rotation about C–N bonds[a]

Compound	Solvent	$\Delta\delta^{b,c}$/Hz	k_c/s^{-1}	T_c/°C	$\Delta G^{\ddagger}$/kcal mol^{-1}
Ia	CD_2Cl_2	11.6	25.8	−5	13.9
Ib[d]	$CDCl_3$	26	58	70	17.4
Id[d,e]	C_5D_5N	40	89	17	14.3
IIb[d]	$CDCl_3$	38	84	90	18.1
IIc[d]	$CDCl_3$	47.0	104	52	16.0
IId[d,e]	$CDCl_3$	40	89	26	14.8
IIIa	$CDCl_3$	53.5	119	27	14.7
IIIc	$CDCl_3$	49.0	109	50	16.0
1	$CDCl_3$	15.0	33.3	10	14.6
3a	CD_2Cl_2	66.5	148	−10	12.7
3b	$CDCl_3$	352	782	27	13.6
3c	$CDCl_3$	178	396	27	14.0
4a	CD_2Cl_2	13.5[f]	30.0	−101	8.7

[a] Some details of calculations and measurements are described in the Experimental section. [b] Measurement on $H^{1,4}$ unless otherwise indicated. [c] 200 MHz NMR for **Ia** and **3c**, for all others 500 MHz. [d] Ref. 2. [e] The measurement corresponds to the nitrogen-inversion barrier. [f] Measurement on $H^{2,3}$.

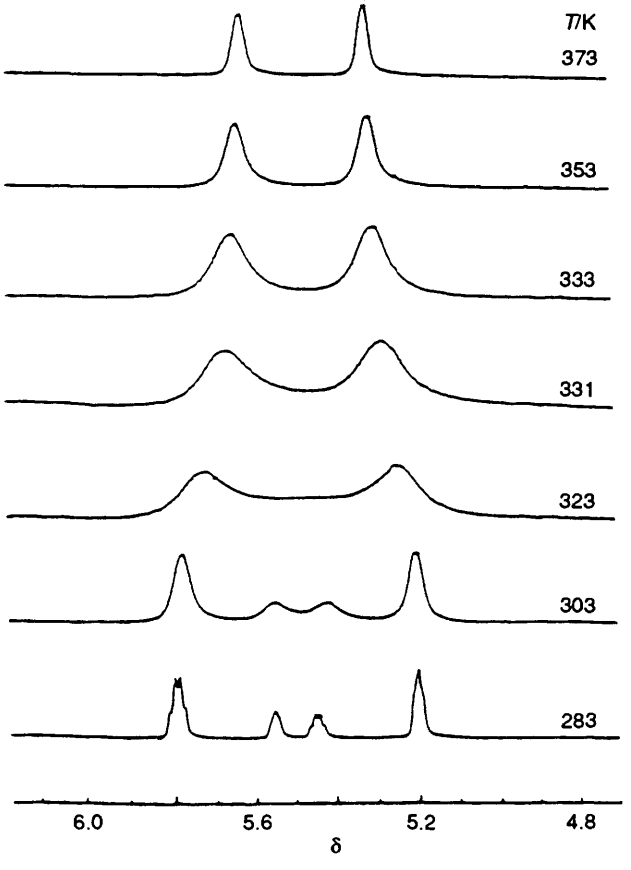

Fig. 1 Variable-temperature ^{1}H NMR spectra for the bridgehead hydrogens of compound **IIIc**. The pair of multiplets at δ 5.2 and 5.8 is derived from one rotamer, that at δ 5.45 and 5.55 from another. The signals coalesce at 523 K

Hindered Rotation in Complexes of 7-Azanorbornadienes.— In previous reports we have found that azanorbornadiene derivatives can co-ordinate to iron carbonyl to form several types of complexes. Typically, the reaction of compound **Ia** with diiron nonacarbonyl produced the tetracarbonyliron complex **1** as primary product. Treatment of **1** with trimethylamine *N*-oxide extrudes one of the co-ordinated CO to yield the tricarbonyliron complex **2**. The lone pair on the nitrogen of **2** contributes to the Fe–N bonding, whereas in **1** there exists only a weak attractive interaction between the nitrogen and one of the CO ligands. For amides the rotational barrier along the C–N bond should be lowered upon N:→Fe co-ordination due to the localization of the lone pair, an effect similar to that of protonation.[9] The free energy of rotation about N–COR of **2** is lower than that of **Ia** as a result of co-ordination. No conformational isomer was observed in the ^{1}H NMR spectrum of **2**, even upon cooling to −40 °C.

The weak attractive force between the nitrogen and CO observed in the crystal of complex **1** is not strong enough to fix the conformation of the carbonyl ligands in solution. Their exchange rate in $CDCl_3$ is high as shown by the singlet observed in the ^{13}C NMR spectrum. However it is quite unexpected to find that the rotational barrier measured for **1** (14.6 kcal mol^{-1}) is higher than that of **Ia** (13.9 kcal mol^{-1}). This enhancement could not be ascribed to the reduction of resonance along the N–COR moiety.

For ordinary anilines such as those in complexes **3** and **4** no rotational barrier along N–Ph is observable at ambient temperature. However, in the ^{1}H NMR spectra of **3b** and **3c** the signals corresponding to the bridgehead hydrogens $H^{1,4}$ appear as broad humps at about δ 5.0–5.5 which can hardly be recognized. In Fig. 2 the spectra of **3b** in the region δ 4.5–8.0 is shown at various temperatures. The Δδ between the bridgehead hydrogens is so large (352 Hz) that at the coalescence temperature (27 °C) the signal can barely be identified against the background. At low temperature the signals can be resolved into pairs of singlets. At below −45 °C the low-field region at

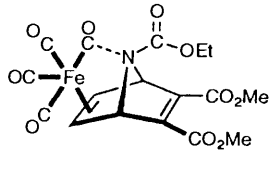

1

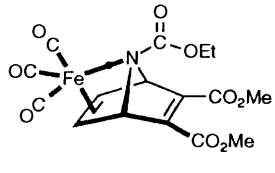

2

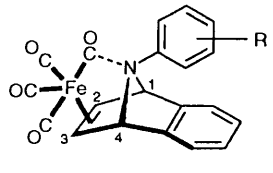

R

3a *o*–Me
3b *o*–CN
3c *o*–I
3d *p*–Me

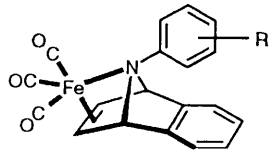

R

4a *o*–Me
4d *p*–Me

δ 6.7–7.6 is also resolved into eight separate signals corresponding to the eight unsymmetrical phenyl hydrogens of the rotamers. The conformational isomerism for the *ortho*-substituted derivatives **3a**–**3c** and **4a** appears as a result of steric hindrance between the phenyl substituents and the co-ordinated CO groups. For *para*-substituted aniline complexes **3d** and **4d** such a barrier does not exist, as can be verified by experiment. As for the isomerism of **1**, the phenomenon can be rationalized by steric interaction in addition to electronic effects.

As shown in Table 1, the rotational barriers measured for complexes **3a** (*o*-methyl), **3b** (*o*-cyano) and **3c** (*o*-iodo) are 12.7, 13.6 and 14.0 kcal mol^{-1} respectively, the ascending order is in accord with the relative size of the substituents. According to the crystal structure of **3d** and the related tetracarbonyliron complexes,[10] the double bond of the 7-aza ring is co-ordinated to the Fe in the equatorial plane of a trigonal-bipyramidal (*TBPY*) co-ordination sphere. The nitrogen atom and the phenyl substituent are located quite close to one of the axial CO groups. For the *ortho*-substituted phenyl derivatives **3a**–**3c**, the rotations along the Fe–(C=C) and N–Ph bonds hamper each other so severely that the hindrance becomes visible in the NMR spectra.

The barrier to rotation observed for complex **4a** is quite low, so that it is necessary to cool the NMR probe to −101 °C in order to examine the coalescence. Compared to **3a**, the distance between Fe and N in **4a** seems to be shorter, hence a higher barrier is expected. However, the experimental result does not seem to agree with such an expectation. The barrier to rotation observed (8.7 kcal mol^{-1}) is actually much lower than that of **3a** (12.7 kcal mol^{-1}). A previous report on the structure of analogous tricarbonyliron complexes[11] indicates that in the *TBPY* geometry of **2** and **4** one of the axial positions originally occupied by CO is taken over by the nitrogen atom. The crowding between N and CO present in **3** is mostly released upon transformation to **4**. To verify our argument, the X-ray crystal diffraction analyses of both **3a** and **4a** were undertaken. The crystal and refinement data are shown in Table 2, whereas atomic coordinates are listed in Tables 3 (**3a**) and 4 (**4a**). Several structural features can readily be recognized from the ORTEP[12] drawings in Figs. 3 and 4. The *N*-phenyl moiety of **3a** (Fig. 3) is not coplanar with C(1)–N–C(4), indicating a weak delocalization along the *n*(N)–π(phenyl) orbitals. The nitrogen atom of **4a** (Fig. 4) occupies one of the axial positions of a *TBPY* co-ordination sphere, so that the *N*-phenyl moiety bends away from the CO ligand as compared with the structure of **3a**.

In the crystalline state the distance measured between the carbons of Ph–CH_3 and Fe–CO is 3.57 Å for complex **3a** and

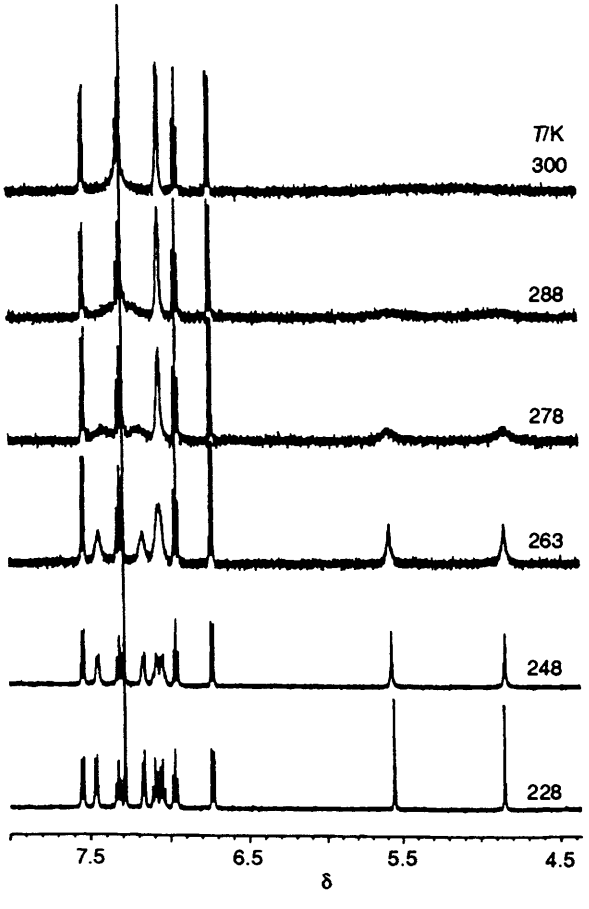

Fig. 2 Variable-temperature ^1H NMR spectra for compound **3b**. The singlets at δ 4.84 and 5.56 are due to the bridgehead hydrogens, whereas those at δ 6.7–7.6 are due to the aromatic ones. The bridgehead signals coalesce at 300 K

Table 2 Crystallographic and refinement data for complexes **3a** and **4a**[a]

	3a	**4a**
Empirical formula	$C_{21}H_{15}FeNO_4$	$C_{20}H_{15}FeNO_3$
M	401.20	373.19
Crystal system	Monoclinic	Triclinic
Space group	$P2_1/n$	$P\bar{1}$
a/Å	9.6938(18)	8.1439(14)
b/Å	19.872(4)	10.4842(16)
c/Å	10.658(3)	10.5792(16)
α/°	90	98.964(13)
β/°	115.498(17)	105.587(12)
γ/°	90	95.951(14)
U/Å^3	1853.1(7)	849.31(23)
Crystal size/mm	0.63 × 0.19 × 0.26	0.38 × 0.07 × 0.25
Z	4	2
F(000)	824	384
D_c/g cm^{-3}	1.438	1.459
μ/mm^{-1}	0.84	0.90
hkl ranges	−10 to 9, 0–21, 0–11	−8 to 8, 0–11, −11 to 11
No. unique reflections	2422	2214
No. observed [$I_o > 2\sigma(I_o)$]	1256	1731
Transmission factors	0.861–1.000	0.876–1.000
Atoms refined	42	40
Parameters	304	286
R^b	0.039	0.032
R'^c	0.041	0.036
Goodness of fit[d]	1.45	1.37
Maximum Δ/σ	0.009	0.167
Electron density/e Å^{-3} maximum and minimum	0.460, −0.230	0.220, −0.180

[a] Details in common: λ 0.7093 Å; $2\theta_{max}$ 45°; scan mode θ–2θ. [b] $\Sigma||F_o| - |F_c||/\Sigma|F_o|$. [c] $[w(|F_o| - |F_c|)^2/\Sigma w|F_o|^2]^{\frac{1}{2}}$. [d] $[\Sigma w(|F_o| - |F_c|)^2/(m - p)]^{\frac{1}{2}}$.

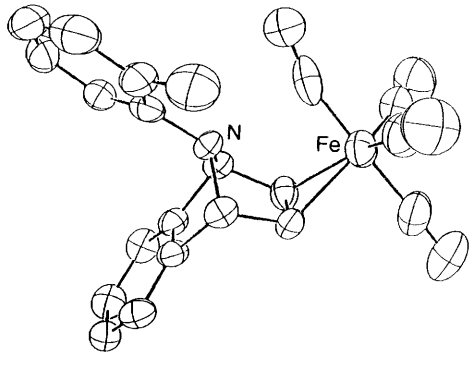

Fig. 3 Perspective drawing of complex **3a**. The numbering scheme is omitted for clarity

Table 3 Atomic parameters and their estimated standard deviations (e.s.d.s) for complex **3a**

Atom	*x*	*y*	*z*	Atom	*x*	*y*	*z*
Fe	0.868 19(12)	0.057 89(5)	0.169 87(11)	C(16)	1.281 9(9)	0.256 4(4)	0.360 1(7)
N	1.103 2(5)	0.165 44(22)	0.342 0(5)	C(17)	1.429 8(11)	0.278 8(5)	0.398 3(8)
O(1)	1.148 6(7)	0.089 6(3)	0.136 4(6)	C(18)	1.549 3(11)	0.236 7(6)	0.464 3(9)
O(2)	1.005 6(9)	−0.071 4(3)	0.288 7(7)	C(19)	1.524 7(10)	0.173 2(6)	0.495 5(9)
O(3)	0.727 0(7)	0.062 6(3)	−0.135 5(6)	C(20)	1.378 3(8)	0.147 2(4)	0.459 8(7)
O(4)	0.577 8(7)	0.016 6(3)	0.170 2(6)	C(21)	1.364 2(14)	0.076 1(5)	0.491 6(13)
C(1)	1.044 5(9)	0.082 3(3)	0.164 4(8)	H(5)	0.752(6)	0.167(3)	0.179(6)
C(2)	0.952 1(10)	−0.022 0(4)	0.241 1(8)	H(6)	0.822(5)	0.102 7(24)	0.385(5)
C(3)	0.781 9(9)	0.059 4(4)	−0.016 7(8)	H(7)	1.112(6)	0.117 1(25)	0.521(5)
C(4)	0.690 6(10)	0.033 3(4)	0.167 4(8)	H(9)	1.024(6)	0.216(3)	0.675(5)
C(5)	0.843 3(8)	0.157 0(3)	0.223 1(7)	H(10)	0.937(6)	0.323(3)	0.682(5)
C(6)	0.889 3(8)	0.116 2(3)	0.341 8(7)	H(11)	0.847(8)	0.377(3)	0.469(7)
C(7)	1.042 6(7)	0.145 8(3)	0.442 9(6)	H(12)	0.871(5)	0.342 0(23)	0.280(5)
C(8)	1.002 5(7)	0.214 2(3)	0.483 2(6)	H(14)	0.982(5)	0.229 6(21)	0.181(4)
C(9)	0.994 2(7)	0.238 9(4)	0.598 9(7)	H(16)	1.202(6)	0.286 9(24)	0.314(5)
C(10)	0.940 6(7)	0.304 1(4)	0.595 9(8)	H(17)	1.440(6)	0.325(3)	0.375(5)
C(11)	0.895 1(8)	0.342 5(4)	0.479 7(8)	H(18)	1.661(8)	0.247(3)	0.500(6)
C(12)	0.901 9(8)	0.317 3(3)	0.359 8(7)	H(19)	1.586(7)	0.142(3)	0.540(6)
C(13)	0.955 0(7)	0.253 9(3)	0.363 2(6)	H(21–1)	1.421(12)	0.054(5)	0.469(11)
C(14)	0.971 0(7)	0.207 7(3)	0.255 1(6)	H(21–2)	1.318(8)	0.068(3)	0.551(7)
C(15)	1.255 4(7)	0.190 8(3)	0.391 1(6)	H(21–3)	1.275(6)	0.053(3)	0.436(5)

Table 4 Atomic parameters and their e.s.d.s for complex **4a**

Atom	*x*	*y*	*z*	Atom	*x*	*y*	*z*
Fe	0.867 07(7)	0.252 75(5)	0.053 15(5)	C(17)	0.808 9(7)	0.156 3(6)	−0.483 0(5)
N	0.727 2(3)	0.236 2(3)	−0.149 7(3)	C(18)	0.772 5(7)	0.024 0(6)	−0.512 1(5)
O(2)	1.209 4(4)	0.267 0(3)	0.008 2(3)	C(19)	0.717 8(7)	−0.040 6(5)	−0.424 5(5)
O(3)	0.800 3(5)	0.008 2(3)	0.146 6(3)	C(20)	0.698 5(5)	0.023 8(4)	−0.303 7(4)
O(4)	1.022 5(4)	0.380 1(3)	0.328 7(3)	C(21)	0.638 1(13)	−0.057 2(6)	−0.216 5(7)
C(2)	1.075 5(5)	0.260 7(3)	0.024 2(4)	H(5)	0.571(4)	0.319(3)	0.083(3)
C(3)	0.821 3(5)	0.097 3(4)	0.098 6(4)	H(6)	0.794(4)	0.495(3)	0.063(3)
C(4)	0.959 8(5)	0.327 4(4)	0.219 6(4)	H(7)	0.855(4)	0.420(3)	−0.154(3)
C(5)	0.632 0(5)	0.314 4(4)	0.020 7(4)	H(9)	0.625(4)	0.561(3)	−0.304(3)
C(6)	0.758 5(5)	0.410 8(4)	0.010 1(4)	H(10)	0.340(4)	0.558(3)	−0.420(3)
C(7)	0.755 4(5)	0.384 8(3)	−0.136 6(3)	H(11)	0.134(5)	0.400(4)	−0.401(4)
C(8)	0.585 3(5)	0.403 8(3)	−0.223 9(3)	H(12)	0.198(5)	0.252(4)	−0.272(4)
C(9)	0.540 8(6)	0.500 9(4)	−0.300 9(4)	H(14)	0.502(4)	0.148(3)	−0.128(3)
C(10)	0.366 9(7)	0.496 0(5)	−0.367 8(4)	H(16)	0.817(5)	0.313(4)	−0.345(4)
C(11)	0.244 1(6)	0.402 0(5)	−0.355 5(4)	H(17)	0.861(6)	0.198(4)	−0.537(5)
C(12)	0.287 9(5)	0.309 8(4)	−0.278 3(4)	H(18)	0.783(6)	−0.032(5)	−0.598(5)
C(13)	0.459 4(5)	0.314 5(3)	−0.212 8(3)	H(19)	0.682(5)	−0.132(4)	−0.442(4)
C(14)	0.553 0(5)	0.232 3(4)	−0.119 3(4)	H(21–1)	0.645(7)	−0.141(5)	−0.250(5)
C(15)	0.738 3(4)	0.159 7(3)	−0.274 9(3)	H(21–2)	0.709(7)	−0.032(5)	−0.134(6)
C(16)	0.792 1(6)	0.224 0(5)	−0.364 8(4)	H(21–3)	0.543(7)	−0.049(6)	−0.194(6)

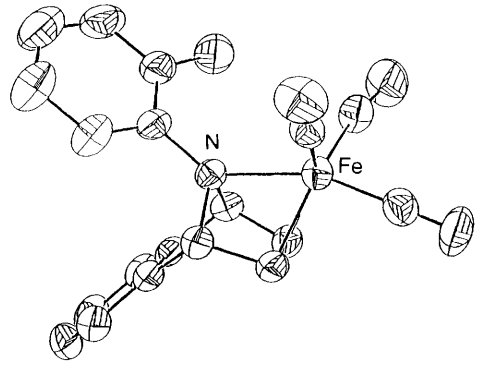

Fig. 4 Perspective drawing of complex **4a**. The numbering scheme is omitted for clarity

3.35 Å for **4a**. The conformation of the methyl substituent is balanced by the surrounding steric environment. In order to estimate the barrier to rotation for the two compounds, a simplified modelling analysis was conducted as follows. Assuming all bond lengths and angles are invariant with respect to the crystal data, a pseudo-rotation along the N–Ph bond was computer simulated. To convert one rotamer into another the methyl group has to squeeze through two energy maxima, *i.e.* the hindrances against the CO ligands in one direction and against the fused benzene moiety in another. For **3a** the estimated shortest distances between the heavy atoms (non-hydrogen atoms) would be 1.51 (between C of methyl and O of CO) and 2.26 Å (C and Ph) respectively, whereas for **4a** the corresponding values would be 2.12 and 2.15 Å. These imply that during rotation along the N–Ph bond of **3a** the most severe barrier appears at the point where the methyl group passes through the CO ligand. Comparatively, the analogous interaction in **4a** is much less significant, and is barely large enough to induce an isomerism on the NMR time-scale at −101 °C.

Structural Parameters.—It has been recognized that the bonding between Fe and N is crucial for the subsequent process of deamination,[13] *i.e.* complex **4** is the intermediate for the fragmentation of **3** to naphthalene. The co-ordination between Fe and N must have a promoting effect for the breakage of N–C(1,4) bonds. According to extended Hückel molecular orbital (EHMO) calculations, the N–C(1,4) bond order in **4** is relatively lower than that in **3**.[14] This reduction in bond order is

Table 5 Selected bond lengths (Å) and angles (°) for complexes **3a**, **3d**, **4a** and **4d**, with e.s.d.s in parentheses

Compound	**3a**	**3d**[a]	**4a**	**4d**[b]
N–C(1)	1.483(7)	1.489(5)	1.530(4)	1.528(3)
N–C(4)	1.477(7)	1.499(5)	1.534(5)	1.521(3)
Fe–C(2)	2.092(7)	2.082(5)	2.014(4)	2.034(3)
Fe–C(3)	2.103(6)	2.085(5)	2.043(4)	2.025(3)
C(1)–N–C(4)	95.6(4)	95.4(3)	93.9(3)	94.1(2)

[a] Ref. 10. [b] Ref. 15.

reflected in the corresponding bond lengths as shown in Table 5. The averaged N–C(1,4) bond length of **4a** (1.532 Å) is *ca.* 0.052 Å longer than that of **3a** (1.480 Å), whereas that of **4d** (1.525 Å) is 0.031 Å longer than that of **3d** (1.494 Å). The elongation of the N–C(1,4) bonds also results in a significant narrowing of the bond angle C(1)–N–C(4), *cf.* **4a** (93.9°) with respect to **3a** (95.6°) and **4d** (94.1°) to **3d** (95.4°). Such changes in bonding parameters, along with other electronic variations,[4] render **3** more susceptible for subsequent nitrene extrusion reactions.

The bonding strains around the metals in complexes **3** and **4** are different as a result of the change in geometry. The Fe–C(2,3) bonds in **4** are considerably shorter than those in **3** (Table 5), indicating a stronger π co-ordination exists in **4**. However, the stronger metal co-ordination does not necessarily imply a longer lifetime of the compound, for the succeeding nitrene extrusion reaction is usually quite rapid.

Conclusion

The hindered rotation observed for complexes **3a**–**3c** and **4a** is caused by steric interference between the phenyl substituents and the co-ordinated CO groups. The magnitude of the free energies ($\Delta G^{\ddagger}$) is directly proportional to the size of the phenyl substituents, *cf.* those of **3a**–**3c** (Table 1), while the barrier is not detectable (by NMR spectroscopy) for the *para*-substituted derivatives such as **3d** and **4d**.

The free energy measured for complex **4a** is lower than that of **3a**, even though the Fe–N bond in the former seems to be shorter. Structural analysis reveals the opposite result, since the CO responsible for the hindrance in **4a** is located at an equatorial position of a *TBPY* co-ordination sphere, whereas that of **3a** is located at an axial position. Computer-simulated rotations along the N–Ph bonds of **3a** and **4a** indicate that the most severe barrier appears at the moment when the methyl group of **3a** passes by the axial CO. This result is consistent with experiment.

Experimental

General.—Proton and ^{13}C NMR spectra were obtained either on a Bruker AMX-500 or an AC-200 FT spectrometer, ^{1}H chemical shifts being measured downfield from $SiMe_4$ while those of ^{13}C were recorded with the central peak of $CDCl_3$ at δ 76.90 as an internal reference. Infrared spectra were recorded on a Perkin Elmer 882 spectrophotometer. Elemental analyses were obtained on a Perkin Elmer 2400 EA instrument. Mass spectra were recorded on a VG Analytical 70-250 S/SE spectrometer. Melting points were measured by a Yanato model MP-S3 MICRO apparatus and were uncorrected.

The azanorbornadiene derivatives **I**,[16] **II**[17] and **III**[18] were synthesised according to the published procedures. The preparation of iron carbonyl complexes[11] and the crystal analyses of **3d**[10] and **4d**[15] have been reported previously.

Variable-temperature Measurements.—Variable-temperature experiments were performed on a Bruker AMX-500 spectrometer using the standard procedure provided by the instrument. Temperatures were not calibrated but before each run the probe was allowed to stabilize for 15 min to the nearest ±0.1 °C. Typically the sample was dissolved in deuteriated solvent and sealed in an NMR tube, then scanned at certain temperature intervals. The coalescence temperature T_c was recorded when the two peaks had just merged. The rate constant k_c was calculated according to the equation $k_c = \pi(\Delta\delta)/2^{\frac{1}{2}}$. The free enthalpy of activation $\Delta G^{\ddagger}$ was deduced from the Eyring equation, where $\Delta G^{\ddagger} = 4.58T_c[10.32 + \log(T_c/k_c)]$.[19]

Tricarbonyl[*7-ethoxycarbonyl-2,3-bis(methoxycarbonyl)-7-azanorbornadiene*]*iron* **2**.—Anhydrous trimethylamine *N*-oxide was prepared according to the literature.[20] To a stirred solution of the tetracarbonyliron complexes **1** * (0.10 mmol) in acetone (50 cm^3) was added NMe_3O (0.20 mmol). The mixture was stirred at room temperature for 2 min, then filtered and dried *in vacuo*. The yield of complex **2** was nearly quantitative. It is not quite stable at room temperature and gradually decomposes in solution; $\nu_{max}(CH_2Cl_2)$ (CO) 2045 and 1965 cm^{-1}; δ_H(500 MHz, $CDCl_3$, −40 °C) 1.18 (3 H, t, J = 7), 3.77 (6 H, s), 4.04 (2 H, q, J = 7 Hz), 4.14 (2 H, s) and 5.52 (2 H, s); δ_C(125 MHz, $CDCl_3$, −40 °C) 29.7, 46.0, 52.9, 64.9, 79.7, 146.9, 155.2, 161.9, 210.4 and 211.7.

Tetracarbonyl- and Tricarbonyl-[*1,4-dihydro*-1,4-(*o-tolylimino*)*naphthalene*]*iron* **3a** *and* **4a**.—To a three-neck round-bottomed flask fitted with a condenser and two dropping funnels was added *N-o*-tolylpyrrole (5.0 g, 3.2 mmol) in tetrahydrofuran (thf) (30 cm^3). The solution was heated to reflux, and from the dopping funnels were added slowly and simultaneously two portions of thf solutions (20 cm^3) of both isopentyl cyanide (2.9 g, 25 mmol) and *o*-aminobenzoic acid (3.3 g, 25 mmol). After the addition the resulting mixture was heated to reflux for 3 h. The solvent was evaporated *in vacuo*, and the product redissolved in CH_2Cl_2. It was washed with 10% NaOH followed by distilled water (50 cm^3 × 2), dried over anhydrous $MgSO_4$, then concentrated. 1,4-Dihydro-1,4-(*o*-tolylimino)naphthalene was purified by passing through a silica gel chromatographic column eluted with hexane–ethyl acetate (5:1 v/v) to collect 2.28 g (0.98 mmol, 31% yield) of product, which was recrystallized from CH_2Cl_2–hexane (Found: C, 87.15; H, 6.65; N, 6.00. Calc. for $C_{17}H_{15}N$: C, 87.50; H, 6.50; N, 6.00%); ν_{max}(KBr) 3069, 3016, 2948, 1578, 1474, 1434 and 1269 cm^{-1}; δ_H(200 MHz, $CDCl_3$) 2.36 (3 H, s), 5.25 (2 H, t, J = 1.3), 6.63–6.67 (1 H, dm, J = 7.5), 6.84–7.05 (6 H, m), 7.07–7.11 (1 H, dm, J = 7.5 Hz) and 7.22–7.27 (2 H, m); δ_C(50 MHz, $CDCl_3$) 18.89, 69.32, 119.83, 120.90, 122.38, 124.63, 125.87, 130.93, 141.28, 144.61 and 149.11; *m/z* (electron impact, EI) 233 (M^+, 100), 217 (37) and 206 (10%).

A two-neck round-bottomed flask fitted with a nitrogen inlet and outlet was purged with nitrogen. 1,4-Dihydro-1,4-(*o*-tolylimino)naphthalene (295 mg, 1.27 mmol), diiron nonacarbonyl (560 mg, 1.54 mmol) and degassed thf (120 cm^3) were added under nitrogen. The solution was magnetically stirred for 18 h at room temperature. It was filtered over Celite and was concentrated *in vacuo*. The iron carbonyl complexes **3a** and **4a** were separated by passing through a silica gel chromatographic column eluted with hexane–ethyl acetate. Their yields were 49 (250 mg, 0.62 mmol) and 15% (71 mg, 0.19 mmol) respectively. Physical data for **3a** (Found: C, 62.50; H, 3.95; N, 3.40. Calc. for $C_{21}H_{15}FeNO_4$: C, 62.85; H, 3.75; N, 3.50%); ν_{max}(KBr) (CO) 2059 and 1961 (br) cm^{-1}; δ_H(200 MHz, $CDCl_3$) 2.26 (3 H, s), 3.58 (2 H, s), 4.78 (2 H, s), 6.56–6.60 (1 H, dm, J = 7.4 Hz), 6.75–6.91 (2 H, m), 6.97–7.08 (3 H, m) and 7.20–7.23 (2 H, m); δ_C(50 MHz, $CDCl_3$) 19.52, 61.63, 66.98, 120.24, 122.40, 123.02, 126.38, 130.17, 131.76, 140.76, 145.58 and 210.28; *m/z* (FAB, ^{56}Fe) 402 (M^+ + 1, 2), 373 (M^+ − CO, 11), 345 (M^+ − 2CO, 24), 317 (M^+ − 3CO, 30), 289 (M^+ − 4CO, 100) and 234 (17%).

* The structure of **5** reported in ref. 11 is revised in ref. 13.

Physical data for **4a** (Found: C, 63.80; H, 4.00; N, 3.80. Calc. for $C_{20}H_{15}FeNO_3$: C, 64.35; H, 4.05; N, 3.75%); ν_{max}(KBr) (CO) 2014, 1945 and 1922 cm^{-1}; δ_H(200 MHz, $CDCl_3$) 2.57 (3 H, s), 4.12 (2 H, s), 6.09 (2 H, s), 6.8–7.0 (3 H, m), 7.09 (2 H, br), 7.13 (2 H, br) and 7.26 (1 H, m); *m/z* (FAB, ^{56}Fe) 373 (M^+, 10), 345 ($M^+ - CO$, 17), 317 ($M^+ - 2CO$, 32), 289 ($M^+ - 3CO$, 100) and 233 (24%).

Tetracarbonyl(1,4-o-*cyanophenylimino*-1,4-*dihydronaphthalene*)*iron* **3b**.—1,4-*o*-Cyanophenylimino-1,4-dihydronaphthalene was synthesised similarly from *N*-(*o*-cyanophenyl)pyrrole (5.0 g, 2.98 mmol) in 48% yield (3.51 g, 1.44 mmol). It was recrystallized from CH_2Cl_2–hexane, m.p. 126–127 °C (Found: C, 83.50; H, 5.15; N, 11.40. Calc. for $C_{17}H_{12}N_2$: C, 83.60; H, 4.95; N, 11.45%); ν_{max}(KBr) (CN) 2214 cm^{-1}; δ_H(200 MHz, $CDCl_3$) 5.66 (2 H, t, J = 1.2), 6.72–6.76 (1 H, d, J = 8), 6.85–6.96 (5 H, m), 7.23–7.36 (3 H, m) and 7.45–7.49 (1 H, dm, J = 8 Hz); δ_C(50 MHz, $CDCl_3$) 69.19, 103.97, 118.66, 119.16, 121.47, 125.06, 133.29, 134.15, 141.76, 147.75 and 149.44; *m/z* (EI) 244 (M^+, 100), 229 (3), 218 (14) and 109 (4%). The tetracarbonyliron complex **3b** was prepared following the procedures described above in 17% yield; ν_{max}(KBr) 2217, 2067 and 1968 (br) cm^{-1}; δ_H(200 MHz, $CDCl_3$) 3.51 (2 H, s), 5.21 (2 H, br), 6.68–6.72 (1 H, d, J = 8), 6.87–6.94 (1 H, t, J = 7.5), 7.00–7.04 (2 H, m), 7.25 (3 H, br) and 7.17–7.51 (1 H, d, J = 7.5 Hz); δ_C(50 MHz, $CDCl_3$) 60.37 (br), 68.03 (br), 104.56, 118.69, 119.79, 122.23, 122.32, 126.55, 133.54, 134.55, 145.42, 146.82 and 209.55; *m/z* (FAB, ^{56}Fe) 413 ($M^+ + 1$, 5), 384 ($M^+ - CO$, 6), 356 ($M^+ - 2CO$, 13), 328 ($M^+ - 3CO$, 43), 300 ($M^+ - 4CO$, 100) and 245 (23%).

Tetracarbonyl[1,4-*dihydro*-1,4-(o-*iodophenylimino*)*naphthalene*]*iron* **3c**.—1,4-Dihydro-1,4-(*o*-iodophenylimino)naphthalene was synthesised from *N*-(*o*-iodophenyl)pyrrole (2.1 g, 0.78 mmol) in 47% yield (1.26 g, 0.365 mmol); ν_{max}(neat) 3055, 3021, 1574, 1453 and 1431 cm^{-1}; δ_H(200 MHz, $CDCl_3$) 5.49 (2 H, t, J = 1.3), 6.58–6.68 (2 H, m), 6.87–6.94 (4 H, m), 7.05–7.13 (1 H, m), 7.21–7.25 (2 H, m) and 7.73–7.78 (1 H, dd, J = 1.4, 7.7 Hz); δ_C(50 MHz, $CDCl_3$) 69.65, 93.29, 120.81, 124.07, 124.49, 128.12, 139.95, 141.11, 146.66 and 148.29; *m/z* (EI) 345 (M^+, 77) 319 (3), 269 (2), 230 (4), 217 (100) and 203 (7%); high resolution mass spectrum required for $C_{16}H_{12}IN$: 345.0015; found: 345.0002. The tetracarbonyliron complex **3c** was prepared by the reaction with $[Fe_2(CO)_9]$ following the above-mentioned procedure, yield 70% (Found: C, 46.50; H, 2.35; N, 2.70. Calc. for $C_{20}H_{12}FeINO_4$: C, 46.80; H, 2.35; N, 2.75%); ν_{max}(KBr) (CO) 2066, 1995 (br) and 1968 (br) cm^{-1}; δ_H(200 MHz, $CDCl_3$) 3.35 (2 H, s), 4.6–5.6 (2 H, br), 6.60–6.63 (2 H, d, J = 7), 7.03 (3 H, br), 7.25 (2 H, m) and 7.74–7.77 (1 H, d, J = 7.5 Hz); δ_C(50 MHz, $CDCl_3$) 67.47, 90.67, 121.68, 122.46, 124.64, 126.41, 128.60, 141.38, 144.26 and 210.25; *m/z* (FAB, ^{56}Fe) 514 ($M^+ + 1$, 1), 485 ($M^+ - CO$, 2), 457 ($M^+ - 2CO$, 8), 429 ($M^+ - 3CO$, 27), 401 ($M^+ - 4CO$, 68), 346 (10), 307 (29) and 289 (17%).

X-Ray Crystallography.—Suitable crystals of complexes **3a** and **4a** were mounted within lithium glass capillaries for data collection on an Enraf–Nonius CAD-4 automated diffractometer. Table 2 gives the crystal data and refinement parameters. Only statistical fluctuations were observed in the intensity monitors over the course of the data collection. An empirical absorption correction based on ψ scans for three reflections near χ = 90° was applied. Coordinates for Fe atoms were obtained from electron-density maps and those of the remaining non-hydrogen atoms from successive Fourier maps. In the final stages, all non-hydrogen atoms were refined anisotropically and all hydrogen atoms were located in a difference map before being refined isotropically to convergence. Following convergence of the original models, the polarity of the space group was checked to ensure a correct choice in the crystallographic chirality. The final difference map was essentially featureless. Atomic scattering factors were taken from ref. 21. The calculation employed a Micro VAX3600 computer using the structure-analysis package developed by NRCC.[22] Molecular drawings of **3a** and **4a** are shown in Figs. 3 and 4.

Additional material available from the Cambridge Crystallographic Data Centre comprises thermal parameters and remaining bond lengths and angles.

Acknowledgements

This work was supported in part by the National Science Council of The Republic of China.

References

1 W. S. Steward and T. H. Siddal, III, *Chem. Rev.*, 1970, **70**, 517.
2 W. J. Deloughry and I. O. Sutherland, *Chem. Commun.*, 1971, 1104.
3 R. C. Newman, jun., and V. Jonas, *J. Am. Chem. Soc.*, 1968, **90**, 1970.
4 L. M. Jackman, T. E. Kavanagh and R. C. Haddon, *Org. Magn. Reson.*, 1969, **1**, 109.
5 A. Rauk, C. A. Leland and K. Mislow, *Angew. Chem., Int. Ed. Engl.*, 1970, **9**, 400; J. M. Lehn, *Fortschr. Chem. Forsch.*, 1971, **15**, 311.
6 W. B. Jennings, S. T. Watson and D. R. Boyd, *J. Chem. Soc., Chem. Commun.*, 1992, 1078.
7 V. Rautenstrauch, *Chem. Commun.*, 1969, 1122.
8 H.-J. Altenbach, D. Constant, H.-D. Martin, B. Mayer, M. Müller and E. Vogel, *Chem. Ber.*, 1991, **124**, 791; K. Yoshikawa, K. Bekki, M. Karatsu, K. Toyoda, T. Kamio and I. Morishima, *J. Am. Chem. Soc.*, 1976, **98**, 3272; I. Morishima, K. Yoshikawa, M. Hashimoto and K. Bekki, *J. Am. Chem. Soc.*, 1975, **97**, 4283; I. Morishima and K. Yoshikawa, *J. Am. Chem. Soc.*, 1975, **97**, 2950; G. R. Underwood and H. S. Friedman, *J. Am. Chem. Soc.*, 1977, **99**, 27; J. B. Grutzner, *J. Am. Chem. Soc.*, 1976, **98**, 6385.
9 P. Hanson and D. A. R. Williams, *J. Chem. Soc., Perkin Trans. 2*, 1973, 2162.
10 L.-K. Liu, C.-H. Sun, C.-Z. Yang, S. Y. Shih, K. S. Lin, Y.-S. Wen and C.-F. Wu, *Organometallics*, 1992, **11**, 972.
11 C. H. Sun, T. J. Chow and L.-K. Liu, *Organometallics*, 1990, **9**, 560.
12 C. K. Johnson, ORTEP, Report ORNL-5138, Oak Ridge National Laboratory, Oak Ridge, TN, 1976.
13 T. J. Chow, J.-J. Hwang, C.-H. Sun and M.-F. Ding, *Organometallics*, 1993, **12**, 3962.
14 H.-W. Huang, S.-L. Lee and T.-J. Chow, *J. Chin. Chem. Soc.*, 1993, **40**, 503.
15 C.-H. Sun and T. J. Chow, *Bull. Inst. Chem. Acad. Sin.*, 1992, **39**, 13.
16 R. Kitzing, R. Fuchs, M. Joyeux and H. Prinzbach, *Helv. Chim. Acta*, 1968, **51**, 888; H. Prinzbach, G. Kaupp, R. Fuchs, M. Joyeux, R. Kitzing and J. Markert, *Chem. Ber.*, 1973, **106**, 3824.
17 C.-H. Sun, C.-Z. Yang, S.-Y. Shih and K.-S. Lin, *Bull. Inst. Chem. Acad. Sin.*, 1991, **38**, 34; L. D. Quin, K. C. Caster, B. G. Marsi and J. A. Miller, *J. Org. Chem.*, 1986, **51**, 3724.
18 H.-J. Altenbach, B. Blech, J. A. Macro and E. Vogel, *Angew. Chem., Int. Ed. Engl.*, 1982, **21**, 778.
19 H. Kessler, *Angew. Chem., Int. Ed. Engl.*, 1970, **9**, 219.
20 J. A. Soderquist and C. L. Anderson, *Tetrahedron Lett.*, 1986, **27**, 3961.
21 J. A. Ibers and W. C. Hamilton (Editors), *International Tables for X-Ray Crystallography*, Kynoch Press, Birmingham, 1974, vol. 4.
22 E. J. Gabe, F. L. Lee and Y. Le Page, The NRC VAX Crystal Structure System, in *Crystallographic Computing 3: Data Collection, Structure Determination, Proteins, and Databases*, eds. G. M. Sheldrick, C. Krueger and R. Goddard, Clarendon Press, Oxford, 1985, pp. 167–174.

Received 27*th August* 1993; *Paper* 3/05188I